Biobased structural epoxy foams derived from plant-oil: Formulation, manufacturing and characterization

Elena Mazzon, Pascal Guigues, Jean-Pierre Habas

Biobased Structural Epoxy Foams Derived from Plant-Oil: Formulation, Manufacturing and Characterization

Elena Mazzon[1], *Pascal Guigues*[2], *Jean-Pierre Habas*[1]*

1 : Institut Charles Gerhardt Montpellier UMR 5253 CNRS-UM-ENSCM, Université de Montpellier, Place Eugène Bataillon, CC 1702, 34095 Montpellier Cedex 5, France

2 : RENFORTECH, 33 Rue de Pierre Marie Fache, 52410 Chamouilley, France

*: Corresponding author

Pr. Jean-Pierre Habas, ICGM, Université de Montpellier, Place Eugène Bataillon, CC 1702, 34095 Montpellier Cedex 5, France.

Tel.: +33 4 67 14 37 80

E-mail address: jean-pierre.habas@umontpellier.fr

ABSTRACT

This paper is devoted to the description of the scientific method used for developing biobased structural foams derived from highly reactive epoxy resins. The chemical formulations were obtained from the mixing of two epoxidized plant oil-derivates (epoxidized linseed oil ELO and glycerol triglycidyl ether commonly named epoxidized glycerol EG) with an anhydride hardener and a non-toxic foaming agent. The optimization of the composition was achieved by studying the influence of many parameters such as the proportion of each epoxy molecule in

the reactive formulation, the exact nature of the hardener or foaming agent retained by the use of different complementary experimental techniques. For instance, the reactivity of four cyclic anhydride compounds with ELO was investigated by differential scanning calorimetry and rheometry in dynamic or kinetic mode. Two different blowing agents were initially retained for the preparation of foams and their respective density and mechanical properties were evaluated and compared. The proportion of each epoxy molecule (ELO and EG) was also tuned to achieve a good equilibrium between the gelation and foaming mechanisms within a few minutes. The definition of an optimized composition made it possible the production of rigid foams using a short production time (i.e. lower than 3 min). These foams were characterized by a glass transition temperature close higher than 80 °C and an apparent density comprised between 0.05 and 0.08 g/cm^3. Their specific mechanical properties were judged convenient for a possible valorisation as lightweight structural material.

KEY WORDS.

Plant-oil derivates; biobased epoxy foam; rheology; anhydride hardener; foaming agent; thermal techniques.

1. INTRODUCTION

Polymer foams define a large range of lightweight materials with very different chemical and physical characteristics that are influenced by the matrix properties, the proportion of the inner cells but also the possible presence of filler in the initial formulation. Polymer foams can be classified into several categories. For instance, they can be separated into either thermoset or thermoplastic materials depending on the nature of the matrix. Each family can be further divided into rigid or flexible substrates. If one considers the spatial repartition of the cells,

isolated gas bubbles are specific of closed-cell foams whereas open-cell structures are based on gas tunnels (Bjork and Enochsson, 2009). Due to all these characteristics, polymer foams can behave as shape memory materials or inversely are able to fulfil structural functions (Lavoie, 1976). Their atypical morphologies provide them outstanding aptitudes for thermal or acoustic insulation. Not surprisingly, given all these properties, these lightweight materials are used in a large range of applications such as building construction (Bogdan et al., 2005; Kallaos et al., 2014; Richardson, 1980), transportation (Farkas et al., 2002; Sakly et al., 2016; Schmitt et al., 2003; Zheng et al., 2011), food packaging (Ingrao et al., 2015; Paraskevopoulou et al., 2012) furniture (Barker et al., 1992; Smardzewski et al., 2008) or sports (Chiu and Shiang, 2007; Duncan et al., 2016).

A general survey shows that most of commercial polymeric foams are derived from petrochemistry. However, for some decades, different elements support the development of biobased foams. First, such materials are really interesting in the framework of a sustainability policy. Indeed, by definition, biomass is renewable whereas crude oil is a fossil resource and so with limited reserves. Secondly, the fluctuating prices of chemicals issued from petroleum is another tangible reason because this makes difficult the choice of long-term technical or scientific solutions (Dvir and Rogoff, 2014). The toxicity of many chemical compounds derived from petroleum chemistry also provides motivation for the identification and use of harmless products. Such situation is found with many conventional types of foams such as polyurethane formulations that are based on isocyanate-functionalised molecules (Avashia et al., 1996; Ganguly et al., 2018; Lee et al., 2003; Pauluhn, 2002). It is also encountered with epoxy foams derived from DiGlycidyl Ether of Bisphenol A (DGEBA). Indeed, Bisphenol A (BPA) was recently suspected to present endocrine disruptor properties but this topic is still subject to controversy (Chen et al., 2002; Resnik and Elliott, 2015; Ruan et al., 2015). The use of other

aromatic prepolymers derived from crude-oil is a possible approach to avoid BPA toxicity but it cannot be considered as a sustainable solution (El Gazzani et al., 2016).

In response to this situation, various studies were undertaken by several teams of researchers to develop epoxy foams from less toxic precursor compounds, in particular through the use of molecules derived from biomass. For instance, Brown et al. explored the interest of a commercial formulation (under trade name Super Sap 100 from Entropy Resins) comprised by epoxidized pine oil and DGEBA and (Brown et al., 2017). Using polymethylhydrosiloxane (PMHS) as a foaming agent in combination with a polyamine hardener, they obtained foams with bulk densities between 0.263 and 0.600 g/cm^3 after curing for 24 hours at ambient temperature. To develop resins with a higher biobased content, Agnihotri used this chemical formulation with variable proportions of epoxidized soya oil ESO (Agnihotri et al., 2019). But, an increase of the ESO content had detrimental impact on both mechanical properties and glass transition temperature of the polymeric foam. Altuna et al. observed similar trend with foams derived from the mixture of DGEBA and ESO (Altuna et al., 2010). This evolution is likely a consequence of the higher molecular flexibility of aliphatic fatty chains compared to rigid aromatic structures present in DGEBA. Generally speaking, epoxidized vegetable oils are known as being characterized by low reactivity due to the poor steric position of oxirane rings in the fatty chains with respect to the hardener (Alam et al., 2014; Biermann et al., 2000; Khot et al., 2001). The time required to produce polymer foams derived from this class of compounds is often several hours and can even be made worse by the choice of the hardener. For instance, Dogan et al. proposed to use malonic acid to cure ESO and act as a blowing agent at the same time. But, they described a slow process and the derived foams were characterized by low performances (Dogan and Kusefoglu, 2008). Nevertheless, in a recent work, we showed that it was possible to produce biobased epoxy foams (i.e. without BPA) within short processing times by using plant-oil derivates and a cycloaliphatic diamine as hardener (Mazzon et al., 2015).

However, due to the excessive exothermicity of the curing reaction, this curing agent also required the addition of other chemicals in the reactive mixture to act as "heat reducer" that is say for preventing thermal runaway. The use of heat reducer made it possible the production of foams. However, the physical characteristics of these foams such low thermomechanical properties (Tg close to 50°C) and excessive density (≈ 0.17 g/cm^3) were judged perfectible considering their possible application in transportation. Then, in this paper, we decided to explore another scientific pathway by the use of cyclic anhydrides that are known to release less heat during their reaction with epoxy molecules (Kumar et al., 2017b). The choice of this kind of hardener was also motivated by the intent to produce foams with higher mechanical properties to fulfil structural applications, in particular for transportation field (Altuna et al., 2015). More precisely, the minimal wished Tg value is about 70 °C whereas the density must be lower than 0.1 g/cm^3. It is important to keep in mind that in this latter sector, the final choice is also oriented towards the formulation able to combine high reactivity during curing and good performances after transformation.

2. EXPERIMENTAL SECTION

2.1 Materials

All raw materials are commercially available and they were used as received, i.e. without further purification. Epoxidized linseed oil (ELO) with 5.8 epoxy groups per triglyceride and molecular weight of 974 g mol^{-1} was kindly offered by ARD (France). Glycerol triglycidyl ether named also epoxidized glycerol (EG) with 3 epoxy groups per molecule and a molecular weight of 260 g mol^{-1} was purchased from Nagase ChemteX (Japan). The chemical structures of these epoxy molecules are drawn in Figure 1.

Insert Figure 1

Different cyclic anhydrides were preselected keeping in mind the wish to get cured materials with good mechanical properties. The different curing agents used in this study are reported in Table 1. All were purchased from Acros Organics and used as received. It is well established by now that the epoxy-anhydride reaction must be catalysed to achieve a full consumption of the reagents and consequently get a material with higher performances. Then, 2-methyl imidazole (2MI) was used as catalyst and was supplied by Sigma Aldrich. $NaHCO_3$ (sodium bicarbonate, "SB") and $KHCO_3$ (potassium bicarbonate, "PB"), purchased from Sigma Aldrich, were used as foaming agent.

Insert Table 1

2.2 Preparation of biobased epoxy resins

All epoxy reactive formulations were prepared with an anhydride groups/epoxy groups ratio R of 0.8 (Boquillon and Fringant, 2000; Gupta et al., 2010). A quantity of 1% wt 2-MI catalyst based on anhydride weight was added to the reactive mixture. For instance, binary mixtures ELO – MTHPA (MTHPA for methyl tetrahydrophthalic anhydride) were characterized by 4.64 mol of hardener for 1 mol of ELO. Ternary formulations are identified under the code "xELO – (100-x)EG – hardener", where x is the percentage of epoxy groups brought by epoxidized linseed oil. Since ELO and EG have a different reactivity with a hardener, these ternary formulations provide the ability to tune the properties of the reactive mixture and the derived material (Habas et al., 2013). Reactive mixtures were prepared in a one-stage process by mixing all chemicals at room temperature under mechanical stirring during 3 minutes until apparent homogeneity. Optimal curing conditions (i.e. time and temperature) were determined by differential scanning calorimetry and rheological analysis.

2.3 Preparation of foams

The epoxy prepolymers were first mixed together in varying proportions but by keeping constant the total number of epoxy groups in order to ensure a complete reaction with the hardener units whatever the formulation studied. Then, the foaming agent was added. Its quantity was fixed between 10 and 50 parts for 100 parts of epoxy formulation corresponding to a weight percentage between 9.1 and 33.3% wt. Finally, the curing agent and the catalyst were also added. All components were mixed at room temperature for about 2-3 minutes. The final blend was poured in an aluminium open mould previously heated at T = 180 °C. The curing/foaming time was set at 3 minutes in order to identify and retain the only formulations compliant with an industrial productivity found in automotive sector.

2.4 Methods

The temperature domains and heat enthalpies attached to the different reactions (i.e. curing of epoxy formulations and decomposition of foaming agents…) were evaluated by differential scanning calorimetry (DSC StarOne from Mettler Toledo®). The dynamic scans were performed with a heating rate of 5 °C min^{-1} under inert atmosphere (N_2) using a 40 µl perforated aluminium capsules and an empty crucible as reference. Kinetic rheological experiments were performed on crude reactive mixtures (i.e. without foaming agent) to determine from the evolution of the complex shear modulus G* = G' + j G" their respective gel and vitrification times. The real component G', called storage modulus, is related to the elastic contribution of the sample. The imaginary part G'', named loss modulus, is specific of the dissipated mechanical energy. These analyses were registered at constant temperature using a dynamic rheometer (MCR 102 from Anton Paar®) equipped with cup-plate geometry. The diameter of the upper plate was 25 mm and the inner diameter of the cup was 40 mm in order to prevent

parasitic side effects. After geometry preheating in the testing chamber up to the desired temperature, the freshly prepared reactive mixture was poured in the measurement cup. Then, the upper plate was lowered until contact with the sample surface. Storage modulus (G') and loss modulus (G'') were recorded at constant strain (5 %) and fixed angular frequency ($\omega = 1$ rad s^{-1}). The gel time was evaluated by taking the time where the divergence of both moduli was observed. The thermomechanical properties of the cured polymer were characterized using a stress-controlled dynamic rheometer (AR2000Ex from TA Instruments®) equipped with rectangular torsion geometry. Analyses were performed from -50 °C to 150 °C with a heating rate of 3 °C min^{-1} and at a constant shearing angular frequency ($\omega = 1$ rad s^{-1}). Glass transition temperature (Tg) was evaluated by taking the temperature $T\alpha$ at the maximum of G'' peak that is characteristic of the main mechanical relaxation. Due to the value of the shearing angular frequency used, $Tg \approx T\alpha$. Dynamic thermogravimetric analyses were performed from room temperature to 300 °C under air flow with the heating rate of 5 °C min^{-1} using a Q50 thermogravimetric analyser (TGA) from TA Instruments®. In isothermal experiments, the weight loss of sample was registered during 60 minutes at a fixed temperature comprised between 100 °C and 180 °C. The density of the foams (ρ) was obtained as the ratio between the weight and the volume of cubes of 25 mm of side. Reported results were the average of measurements taken on three different samples issued from the same chemical formulation. Dynamic mechanical analyses (DMA) of the foams were performed with a 50N model from ACOEM-Metravib® using parallel plate geometry in compressive mode at a constant frequency (1 Hz). The temperature ranged from -50 °C and 130 °C with a heating rate of 2° C min^{-1}. Glass transition temperature (Tg) of the foam was evaluated by taking the temperature at the maximum of peak on E'' curve. This temperature also corresponds to the beginning of the drop of the Young's modulus plot that is characteristic of the mechanical rigidity. The compressive performances of the foam were also evaluated at room temperature

on cubic samples (20 mm x 20 mm x 20 mm) using a 5533 Universal Testing Machine from Instron® with a crosshead speed of 5 mm min^{-1}. The compressive modulus was determined from the slope of stress – strain curve in linear region associated with the elastic behaviour. The compressive strength was taken at a strain of 10 %. Reported results were the average of at least eight measurements on specific samples.

3. RESULTS AND DISCUSSION

3.1 Choice of anhydride hardener

The reactivity of ELO with each kind of anhydride hardener was first investigated with dynamic DSC. The crosslinking thermal domain was detected by the presence of an exothermic peak (Figure 2). Its position and respective area were observed to be slightly different form one anhydride to other. The peak characteristic of the reaction between ELO and MHHPA (methyl hexahydrophthalic anhydride) units presented a maximum centred at the lowest temperature (i.e. T = 150 °C) and was judged as specific of the most reactive mixture. The reverse situation (i.e. lowest reactivity) was observed with the use of METH (nadic methyl anhydride) hardener. Such hierarchy was found consistent with literature data (Boquillon and Fringant, 2000).

Insert Figure 2

Then, kinetic rheological analyses could be recorded for each reaction mixture at different constant curing temperatures taken in the thermal crosslinking range defined above. In particular, the divergence of both viscoelastic moduli was used to evaluate the gel time. Figure 3 shows the gel times characteristic of the four couples "ELO-anhydride" registered at T = 80 °C and 140 °C, respectively. At the lowest curing temperature, the mixtures based on THPA (tetrahydrophthalic anhydride), MTHPA and MHHPA have similar reactivity with gel

times close to 200 minutes. In contrast, epoxy formulation based on METH is considerably less reactive since its gel time close to 350 minutes. The same hierarchy is observed at high temperature (T = 140 °C). The lower reactivity of METH is likely a consequence of its bulky nadic structure synonym of reduced molecular mobility (Table 1).

Insert Figure 3

The thermomechanical properties of "ELO – anhydride" cured materials were evaluated by dynamic rheology. Figure 4 resumes glass transition temperature values after curing at T = 80 °C during 24 hours or at T = 140 °C during 10 hours. After curing at T = 80 °C, the formulations with the highest Tg are ELO – MHHPA and ELO – MTHPA (75 °C and 73 °C respectively). This result is not surprising since MTHPA and MHHPA show very similar chemical structures and reactivity. In contrast, the lowest value (30 °C) is obtained with the ELO – METH formulation. Such result can be once more related to the lower reactivity of this system. In this latter case, a curing time of 24 hours seems insufficient for the total consumption of reactive compounds. A temperature increase to T = 140 °C provides a higher crosslinking rate. Then, the Tg of ELO – METH formulation is close to that registered with ELO – MHHPA and ELO – MTHPA cured materials. It is to note that the cured material based on ELO – THPA displays the lowest Tg values for both curing temperatures used. Considering that THPA anhydride is under solid state up to 102 °C, its use is less practical than liquid anhydrides such as MHHPA and MTHPA. As the latter offer the best combination between reactivity and ultimate performances, they will be the only anhydrides retained in the pursuing of our work. In fact, only results related to formulations derived from anhydride MTHPA are presented because those registered with MHHPA are very little different.

Insert Figure 4

3.2 Study of ternary formulations

Dynamic DSC analyses were performed on several "xELO – (100-x)EG – MTHPA" ternary formulations in order to evaluate the temperature domains attached to the curing reaction. The corresponding thermograms are presented in Figure 5. The binary ELO – MTHPA and EG – MTHPA formulations exhibit specific exothermic reactions peaks attributed to the epoxy – anhydride curing reaction. In case of reactive mixture based on ELO, the crosslinking reaction starts at high temperature ($T \approx 80$ °C) and ends at 250 °C. The use of EG in place of ELO shifts the reaction domain to lower temperature. Indeed, the reaction between EG and MTHPA produces itself from 25 °C to 160 °C. This evolution is ascribed to higher accessibility of oxirane groups to anhydride functions (Alam et al., 2014; Biermann et al., 2000; Habas et al., 2013; Khot et al., 2001). The calorimetric response of ternary mixtures is characterized by the presence of two partially overlapped exothermic peaks, the intensities of which are more or less pronounced according to the initial composition of the formulation. They are easily attributable to EG – MTHPA reactions for the lowest temperatures and to ELO – MTHPA for the highest. A similar behaviour was already observed in the literature for systems based on "DGEBA – epoxidized soybean oil – MTHPA" with increasing amounts of DGEBA (Altuna et al., 2011).

Insert Figure 5

The total specific enthalpy of reaction (ΔH, in J g^{-1}) can be evaluated by direct integration of the exothermic peaks. Then, it clearly appears that the progressive substitution of ELO by EG in the reaction mixture provokes a slight increase of the released heat (Figure 6). Indeed, the

discrepancy between the extreme values corresponding respectively to ELO – MTHPA and EG – MTHPA formulations remains limited (about 30 J g^{-1}) while the maximal value of enthalpy does not exceed 350 J g^{-1}. In that sense, this behaviour is quite different from that observed in the case of epoxy ternary formations based on ELO, EG and an amine hardener (Mazzon et al., 2015). Indeed, in this latter case, the crosslinking enthalpy was observed to strongly increase with the EG content in the formulation. This evolution has been explained and related to the parasitic consumption of amine functions by ester functions only present in ELO. Such unwished reaction named "amidation" and described in other papers is not possible here due to the nature of the hardener (Del Rio et al., 2011; Lee et al., 2008; Liu et al., 2005). It is important to keep in mind that in the present study, the highest enthalpy value is well below the minimal value above which the self-combustion of the sample cured with the diamine was observed. In other words, anhydride-based formulations offer more comfortable and safe manufacturing conditions.

Insert Figure 6

Kinetic rheological experiments were performed at different constant temperatures to evaluate the gel time of each formulation but also the minimum time required for the complete consumption of all reactive components. Figure 7a shows the evolution of complex shear modulus G* = G' + j G'' of 80ELO – 20EG – MTHPA formulation as a function of time and at two constant temperatures T = 80 °C and 140 °C. At the beginning of both analyses, moduli G' and G'' have low values with G'' > G'. This means that the reactive mixture is still in the liquid state and the reaction advancement remains limited. Then, the formation of a percolating network induces the gelation of the system revealed by a sudden increase of both moduli. The time related to this strong evolution is used to evaluate the gel time of the medium. As showed

before with calorimetry, a temperature increase boosts reactivity and a reduction of gel time. After the gel point, the densification of the polymeric network provokes the pursuing of both moduli increase. Then, the viscoelastic curves tend to a limit allowing the definition of the minimal period required to achieve the curing reaction at the temperature used during the experiment. Figure 7b presents the different gel times registered at T = 80 °C and 140 °C for several ternary formulations. Whatever the curing temperature is, the progressive replacement of ELO by EG induces a reduction in gel time. Similar tendency is observed with the vitrification time. These evolutions agree with the conclusions proposed after examination of the DSC experiments. Compared to ELO molecules, EG units are more reactive with MTHPA because they combine more accessible epoxy groups with higher molecular mobility. As mentioned in introduction of this research, epoxy resins with high reactivity are often good candidates for possible application in industry. Seen from this perspective, the most interesting formulations are undeniably those with high amounts of EG because they present a gel time significantly lower than 3 minutes as required for the wished industrial application.

Insert Figure 7

The thermomechanical properties of cured materials were investigated by dynamic rheology. The analysis characteristic of the 10ELO – 90EG – MTHPA formulation after complete curing is presented as example in Figure 8a. At low temperatures, the cured material is in the glassy state. It is rigid and the storage modulus G' displays high values (G' > 1 GPa). Then, in the "transition zone" the value of G' sharply decreases in a limited temperature range. Simultaneously in the same area, the loss modulus G'' describes a peak commonly called "α peak" that is characteristic of the mechanical relaxation of polymeric network during the glass transition. Taken at its maximum, the Tα temperature is evaluated close to 70 °C. Above

the glassy transition, the sample is in rubbery state. The storage modulus G' is still predominant but its values are two decades lower than in the glassy state. Figure 8b resumes the Tg values for several cured materials based on "xELO – (100-x)EG – MTHPA" reactive mixtures. These data reveal that the glass transition temperature of the cured material is poorly dependent on the respective proportions of ELO and EG in the initial reactive mixture.

Insert Figure 8

A possible explanation for this behavior can be found by examining the structure of the network formed during curing. The smaller size of EG compared to ELO would suggest higher crosslinking density, so higher final properties for cured materials with high amount of EG. But in ELO, oxirane functions derived from epoxidation of native double bonds are much close to each other. Each epoxy cycle is able to establish two covalent bonds with anhydride units. So the distance between crosslinking points in cured network based on ELO is potentially lower than in those based on EG. Figure 9a shows a schematic representation of an "ELO – anhydride (A)" crosslinked structure, with different mesh sizes: 1) based on close epoxy groups and 2) including "glycerol" core.

Insert Figure 9

The introduction of an increasing proportion of EG in the reactive formulation should increase the density of the network due to the smaller size of the epoxy prepolymer. But mesh size could be larger (Figure 9b). In conclusion mesh average sizes in "ELO – anhydride" and "EG – anhydride" are likely to be equivalent what could justify that the initial composition has slight influence on glass transition temperatures. Such hypothesis seems to be supported by the

direct comparison of the thermomechanical profiles of two cured materials (Figure 8a), the former being rich in ELO, the latter in EG. In the rubbery plateau, both cured formulations present almost the same value of the storage modulus. According to the law of rubber elasticity, this means that the crosslink densities of these materials are quite close (Everaers and Kremer, 1995; Treloar, 1975).

3.4 Characterization of foaming agents

In order to produce polymeric thermosetting foams within short period, a polymeric formulation rich in EG must be retained. Then, the formulation 10ELO – 90EG – MTHPA characterized by very short gel times (i.e. close to 1 minute at T = 140 °C) and good thermomechanical properties after curing (Tg > 70 °C), was selected. According to the method proposed by Pan (Pan et al., 2011) the biobased content of this reactive mixture is about 38.6 %. A foam production from a polymer matrix requires the addition of a blowing agent but its choice is not trivial since a good equilibrium between the gas emission and the crosslinking reaction is indispensable (M. O. Okoroafor, 1995; Mazzon et al., 2015; McElhanon et al., 2002; Takiguchi et al., 2008). Among the different possible chemical agents, we decided to investigate the interest of sodium bicarbonate ($NaHCO_3$, SB) and potassium bicarbonate ($KHCO_3$, PB). Indeed, upon heating, these non-toxic compounds decompose producing carbon dioxide and water in gaseous state (Scheme 1).

Insert Scheme 1

The range associated with the thermal decomposition of both bicarbonates was investigated by thermogravimetric analysis in dynamic mode. Sodium bicarbonate decomposes between 80 °C

and 190 °C while the thermal decomposition of potassium bicarbonate is observed at higher temperature between 100 °C and 195 °C (Figure 10).

Insert Figure 10

In both cases, a significant residual weight is observed, the value of which (63 % for SB and 69% for PB) agrees with the reaction scheme (i.e. production of Na_2CO_3 and K_2CO_3). To evaluate which blowing agent is the most adequate with the reactive polymeric formulation, we reported in Figure 11 the calorimetric behaviours of the reactive formulation 10ELO – 90EG – MTHPA and those of SB and PB. All these experiments were recorded in the same conditions. The crosslinking reaction is detected through the presence of an exothermic peak while the respective decompositions of the blowing agents appear as endothermic phenomena. At first sight, the use of SB seems to be preferable instead of PB because its decomposition thermal range overlaps in a better way with that specific of the resin curing.

Insert Figure 11

But, other aspects must be considered such as the evolution of the resin viscosity with temperature confronted with the gas generation. Figure 12 shows the viscosimetric profile of the pure reactive mixture superimposed with the derivative of weight loss curve of each foaming agent registered with the same heating ramp. The gelation of the only resin detected by the divergence of the viscosity occurs in a temperature range for which SB start to decompose. At first sight, this situation may appear ideal for the foaming process since the bubbles are likely to be trapped (Hwang et al., 1994; McElhanon et al., 2002; Tungare et al., 1988). Nevertheless, practical trials revealed that the crosslinking process is delayed when SB is added to the initial

resin. An apparent lack of curing is even observed since the resin is still sticky. These unwished characteristics are likely provoked by the heat consumption during SB decomposition and so, a reduction of the real curing temperature. Further possible factor is the production of water molecules that consume anhydride molecules what affects the wished epoxy-hardener reaction. Then, it appears that the blowing agent decomposition should take place in the last part of the thermal domain characteristic of the resin curing so as to limit the parasitic influence of the endothermic gas production on the temperature-activated crosslinking reaction.

Insert Figure 12

Both Figures 11 and 12 show that such situation is encountered with the use of potassium bicarbonate. Then, this latter compound was finally retained as foaming agent in order to produce lightweight rigid foams.

In order to evaluate the kinetics of PB decomposition, different isothermal thermogravimetric analyses of this compound were registered for temperatures comprised between 80 °C and 180 °C. The corresponding data presented in Figure 13 demonstrate that the decomposition rate increase with temperature. A process temperature of 180 °C seems adequate for the complete gas production in very short delays.

Insert Figure 13

3.5 Characterization of final materials

Trials for production of macroscopic epoxy foams were undertaken at T = 180 °C with a fixed time of 3 minutes. The amount of foaming agent ranged from 10 to 70 parts for 100 parts of epoxy formulation, corresponding to a weight percentage comprised between 9.1 and 41.1%

wt. Figure 14a clearly shows that the introduction of 10 parts of BP produces compact samples due to a quite reduced foaming process. Then, it is observed that that the final volume of the foam increases with the initial quantity of PB. But, please note that for PB amounts higher than 50 parts, the foam is made with big inner bubbles and is even quite brittle. Our trials lead to the conclusion that the highest value of PB amount is 50 parts. In this case, the gas production self-stops after 3 minutes at T = 180 °C and the expansion is quite acceptable.

Insert Figure 14

Figure 14b resumes apparent density of prism-shaped samples cut in the core of each foam for an initial PB comprised 20 and 50 parts. All registered values are lower than 0.10 g/cm^3. However, a big dispersion of density values is observed with the materials containing 20 parts of PB and is probably a consequence of the samples heterogeneity before cutting process. The apparent density decreases with an increasing amount of foaming agent and a better reproducibility is obtained for the foams produced with the higher PB amounts.

The same foams were also characterized by dynamic mechanical analysis in compressive mode and as a function of temperature. Above a critical temperature, the E' curve decreases faster due the material transition from the glassy state to the rubbery state. This critical temperature provides a good evaluation of the Tg of the polymer matrix due to the value of the compressive frequency used for this thermomechanical analysis (f = 1 Hz) (Chen et al., 2014; McElhanon et al., 2002; Sankaran et al., 2006). The exploitation of DMA results is resumed in Figure 15. The Tg of the different foams is comprised between 80 and 87 °C. Then, it seems not to be dependent on the amount of PB present in the initial mixture as found by Stefani with another kind of epoxy foam (Stefani et al., 2003). Please note that this Tg value is higher than the minimal value required for the wished application for all formulations studied.

Insert Figure 15

This point is particularly important because the first tests conducted with sodium bicarbonate revealed that this blowing agent significantly affected the foam thermomechanical properties by consuming heat at the expense of the resin crosslinking degree. In other words, by decomposing at higher temperature PB seems once more a better choice with our epoxy formulation.

To complete the mechanical characterisation section, compressive tests were also performed with the different foams produced with a PB content comprised between 20 and 50 parts Figure 16a depicts as example a typically stress–strain curve registered on a sample obtained with 30 parts of PB. This curve can be roughly divided into three different zones. The first one is characterized by a linear evolution of stress with strain. It corresponds to the linear elastic domain. It allows the evaluation of the "apparent" Young's modulus of the foam, mainly related to the mechanical rigidity of cells walls. In the second zone, the collapse of cells walls induces the formation of a plateau-like region in the stress–strain curve. The compressive strength (σc) is measured at 10 % strain for further comparison between all samples. Finally, at higher strain, opposed cell walls touch each other what induces a strong increase of the curve. This last step is usually named "densification" (Avalle et al., 2001; Deschanel et al., 2009; Gibson and Ashby, 1982; Greco and Lionetto, 2009; Pampolini, 2010). Figure 16b summarizes the results of all compressive tests. These data reveal that the compression modulus value decreases with the amount of foaming agent. The same trend is also observed for the compressive strength. However, the foams produced with 20 parts of PB are characterized by a big dispersion of their mechanical compressive properties, probably due to their poor homogeneity. These results perfectly agree with density data presented above. Indeed, the gradual transition from a solid

material to a cellular structure induces a classical reduction in compressive mechanical properties. The same evolution was observed by Altuna (Altuna et al., 2015) in case of polymeric foams based on epoxidized soybean oil and MTHPA hardener. According to the classification proposed in literature (Basso et al., 2011; Guo et al., 2000) foams with 20 and 30 parts of PB are defined as "rigid" while those obtained with 40 and 50 parts of foaming agent are "semi-rigid".

Insert Figure 16

Compared to the previous materials derived from the same epoxy compounds but using isophorone diamine as hardener and SB as blowing agent (Mazzon et al., 2015), this new family of foams offers real added value. In particular, due to the reduced exothermicity of the crosslinking reaction, it does not require the use of any additive acting as heat absorber on the opposite of the first generation. Moreover, the ultimate properties of the foams described here are significantly superior to those previously described. For instance, the final Tg is 30°C higher while the mechanical rigidity is increased by nearly 60%. It is important to note that these improvements were not obtained at the expense of the density since in this research, it was comprised between 0.05 and 0.08 g/cm^3 against 0.17 g/cm^3 for the best candidate developed in our previous study. Considering biobased epoxy foams produced from other resources, it is worthy to note that the Tg of our materials are significantly higher than that obtained by Khundamri and al. (close to -6 °C) with foams synthesized from various mixtures of epoxidized soybean oil (ESO) and epoxidized mangosteen tannin cured with the same hardener (MTHPA) used in our research (Khundamri et al., 2019). In this latter case, the absence of catalyst in the reactive formulation but also the lower functionality of ESO (Kumar et al., 2017a) are likely at the origin of this discrepancy. The macroscopic properties of our optimal foam are also

significantly higher than those recently described by Agnihotri et al. with a foam produced from the mixture of ESO, epoxidized pine oil and DGEBA with polyamines as hardener. Indeed, in this study the maximal Tg is close to 56 °C while the minimal density is 0.53 g/cm^3 (Agnihotri et al., 2019). The elimination of ESO in the formulation to the benefit of DGEBA is a good way for increasing the thermomechanical properties since the Tg rises up to 97 °C. But, the time required for the curing (24 h) remains much higher than that described here. In our study, the controlled addition of EG to ELO made it possible the reduction of the process time to 3 minutes. This approach offers a real implementation of the solution explored by Altuna et al. from the mixture of ESO, MTHPA and SB since in this last case, gel times higher than 20 minutes are reported (Altuna et al., 2015).

4. CONCLUSIONS

This work shows that it is possible to produce epoxy foams for a structural purpose in a few minutes using different chemical compounds derived from plant-oil and an inert blowing agent. The proposed methodology emphasizes that several factors must be considered such as the thermal domains associated with the crosslinking of the polymer formulation and the decomposition of the blowing agent respectively. Based on our results, it is preferable to choose a blowing agent the action of which occurs when the crosslinking has already reached an advanced stage. Indeed, it is possible to trap the gas produced in the gelled polymer matrix without affecting its cross-linking degree. In addition, the kinetics associated with each of these phenomena must be carefully determined. In our study, the low reactivity of an epoxidized vegetable oil is compensated by the use of epoxidized glycerol that presents oxirane groups more accessible to the hardener units. This study also underlines that the use of several experimental techniques is of first importance to identify the most performing formulation. The best one is based upon the 10ELO – 90EG – MTHPA reactive mixture and ideally contains 30

parts of PB for 100 parts of resin (⇔ 23.1% w/w). After 3 min of curing at T = 180 °C, the foam derived from this formulation combines good mechanical performances (Tg > 80 °C, high mechanical rigidity) with a quite low density (0.065 g/cm^3). Such mixture allows the description of short processing times thus meeting the requirements of an industrial production line. All these scientific elements but also the raw materials prices and their factual availability make it realistic a possible valorisation of this plant-oil based formulation for producing foams at larger scale.

REFERENCES

Agnihotri, S., Shukla, S., Pradeep, S.A., Pilla, S., 2019. Biobased thermosetting cellular blends: Exploiting the ecological advantage of epoxidized soybean oil in structural foams. Polymer 177, 111-119.

Alam, M., Akra, D., Sharmin, E., Zafar, F., Ahmad, S., 2014. Vegetable oil based eco-friendly coating materials: A review article. Arabian Journal of Chemistry 7, 469-479.

Altuna, F.I., Esposito, L., Ruseckaite, R.A., Stefani, P.M., 2010. Syntactic foams from copolymers based on epoxidized soybean oil. Composites Part A-Applied Science and Manufacturing 41, 1238-1244.

Altuna, F.I., Esposito, L.H., Ruseckaite, R.A., Stefani, P.M., 2011. Thermal and Mechanical Properties of Anhydride-Cured Epoxy Resins with Different Contents of Biobased Epoxidized Soybean Oil. Journal of Applied Polymer Science 120, 789-798.

Altuna, F.I., Ruseckaite, R.A., Stefani, P.M., 2015. Biobased Thermosetting Epoxy Foams: Mechanical and Thermal Characterization. ACS Sustainable Chemistry & Engineering 3, 1406-1411.

Avalle, M., Belingardi, G., Montanini, R., 2001. Characterization of polymeric structural foams under compressive impact loading by means of energy-absorption diagram. International Journal of Impact Engineering 25, 455-472.

Avashia, B., Battigelli, M.C., Morgan, W.K.C., Reger, R.B., 1996. Effects of prolonged low exposure to methyl isocyanate. Journal of Occupational and Environmental Medicine 38, 625-630.

1 Barker, M., Hannaby, M.P., Lockwood, F.J., 1992. Combustion modified molded polyurethane
2 flexible foam for the furniture industry. Cellular Polymers 11, 83-95.

3 Basso, M.C., Li, X., Fierro, V., Pizzi, A., Giovando, S., Celzard, A., 2011. Green,
4 formaldehyde-free, foams for thermal insulation. Advanced Materials Letters 2, 378-382.

5 Biermann, U., Friedt, W., Lang, S., Luhs, W., Machmuller, G., Metzger, J.O., Klaas, M.R.,
6 Schafer, H.J., Schneider, M.P., 2000. New syntheses with oils and fats as renewable raw
7 materials for the chemical industry. Angewandte Chemie-International Edition 39, 2206-2224.

8 Bjork, F., Enochsson, T., 2009. Properties of thermal insulation materials during extreme
9 environment changes. Construction and Building Materials 23, 2189-2195.

10 Bogdan, M., Hoerter, J., Moore, F.O., 2005. Meeting the insulation requirements of the building
11 envelope with polyurethane and polyisocyanurate foam. Journal of Cellular Plastics 41, 41-56.

12 Boquillon, N., Fringant, C., 2000. Polymer networks derived from curing of epoxidised linseed
13 oil: influence of different catalysts and anhydride hardeners. Polymer 41, 8603-8613.

14 Chen, K., Tian, C., Lu, A., Zhou, Q., Jia, X., Wang, J., 2014. Effect of SiO_2 on Rheology,
15 Morphology, Thermal, and Mechanical Properties of High Thermal Stable Epoxy Foam.
16 Journal of Applied Polymer Science 131, 1-7.

17 Chen, M.Y., Ike, M., Fujita, M., 2002. Acute toxicity, mutagenicity, and estrogenicity of
18 bisphenol-A and other bisphenols. Environmental Toxicology 17, 80-86.

19 Chiu, H.T., Shiang, T.Y., 2007. Effects of insoles and additional shock absorption foam on the
20 cushioning properties of sport shoes. Journal of Applied Biomechanics 23, 119-127.

1 Del Rio, V., Callao, M.P., Larrechi, M.S., 2011. Analysing the Temperature Effect on the
2 Competitiveness of the Amine Addition versus the Amidation Reaction in the Epoxidized
3 Oil/Amine System by MCR-ALS of FTIR Data. International Journal of Analytical Chemistry
4 2011, 1-10.

5 Deschanel, S., Vanel, L., Godin, N., Maire, E., Vigier, G., Ciliberto, S., 2009. Mechanical
6 response and fracture dynamics of polymeric foams. Journal of Physics D-Applied Physics 42,
7 1-14.

8 Dogan, E., Kusefoglu, S., 2008. Synthesis and in situ foaming of biodegradable malonic acid
9 ESO polymers. Journal of Applied Polymer Science 110, 1129-1135.

10 Duncan, O., Foster, L., Senior, T., Alderson, A., Allen, T., 2016. Quasi-static characterisation
11 and impact testing of auxetic foam for sports safety applications. Smart Materials and Structures
12 25.

13 Dvir, E., Rogoff, K., 2014. Demand effects and speculation in oil markets: Theory and
14 evidence. Journal of International Money and Finance 42, 113-128.

15 El Gazzani, S., Nassiet, V., Habas, J.P., Freydier, C., Hilleshein, A., 2016. High Temperature
16 Epoxy Foam: Optimization of Process Parameters. Polymers 8.

17 Everaers, R., Kremer, K., 1995. TEST OF THE FOUNDATIONS OF CLASSICAL RUBBER
18 ELASTICITY. Macromolecules 28, 7291-7294.

19 Farkas, P., Stanciu, R., Mendoza, L., 2002. Automotive, molded viscoelastic foams. Journal of
20 Cellular Plastics 38, 341-354.

Ganguly, B.B., Mandal, S., Kadam, N.N., 2018. Spectrum of health condition in methyl isocyanate (MIC)-exposed survivors measured after 30 years of disaster. Environmental Science and Pollution Research 25, 4963-4973.

Gibson, L.J., Ashby, M.F., 1982. The mechanics of three-dimensional cellular materials. Proceedings of Royal Society of London, Series A 382, 43-59.

Greco, A., Lionetto, F., 2009. The Influence of the Stress Relaxation and Creep Recovery Times on the Viscoelastic Properties of Open Cell Foams. Polymer Engineering and Science 49, 1142-1150.

Guo, A., Javni, I., Petrovic, Z., 2000. Rigid polyurethane foams based on soybean oil. Journal of Applied Polymer Science 77, 467-473.

Gupta, A.P., Ahmad, S., Dev, A., 2010. Development of Novel Bio-Based Soybean Oil Epoxy Resins as a Function of Hardener Stoichiometry. Polymer-Plastics Technology and Engineering 49, 657-661.

Habas, J.-P., Lapinte, V., Ulloa, H.A., Giani, O., WO2013124574, 2013.

Hwang, J.G., Row, C.G., Hwang, I., Lee, S.J., 1994. A Chemorheological Study on the Curing of Thermosetting Resins. Industrial & Engineering Chemistry Research 33, 2377-2383.

Ingrao, C., Lo Giudice, A., Bacenetti, J., Khaneghah, A.M., Sant'Ana, A.D., Rana, R., Siracusa, V., 2015. Foamy polystyrene trays for fresh-meat packaging: Life-cycle inventory data collection and environmental impact assessment. Food Research International 76, 418-426.

Kallaos, J., Bohne, R.A., Hovde, P.J., 2014. Long-Term Performance of Rigid Plastic Foam Building Insulation. Journal of Materials in Civil Engineering 26, 374-378.

Khot, S.N., Lascala, J.J., Can, E., Morye, S.S., Williams, G.I., Palmese, G.R., Kusefoglu, S.H., Wool, R.P., 2001. Development and application of triglyceride-based polymers and composites. Journal of Applied Polymer Science 82, 703-723.

Khundamri, N., Aouf, C., Fulcrand, H., Dubreucq, E., Tanrattanakul, V., 2019. Bio-based flexible epoxy foam synthesized from epoxidized soybean oil and epoxidized mangosteen tannin. Ind. Crop. Prod. 128, 556-565.

Kumar, S., Samal, S.K., Mohanty, S., Nayak, S.K., 2017a. Epoxidized Soybean Oil-Based Epoxy Blend Cured with Anhydride-Based Cross-Linker: Thermal and Mechanical Characterization. Industrial & Engineering Chemistry Research 56, 687-698.

Kumar, S., Samal, S.K., Mohanty, S., Nayak, S.K., 2017b. Study of curing kinetics of anhydride cured petroleum-based (DGEBA) epoxy resin and renewable resource based epoxidized soybean oil (ESO) systems catalyzed by 2-methylimidazole. Thermochimica Acta 654, 112-120.

Lavoie, F.J., 1976. Structural foam in transportation industry. Journal of Cellular Plastics 12, 320-&.

Lee, C.T., Friedman, M., Poovey, H.G., Ie, S.R., Rando, R.J., Hoyle, G.W., 2003. Pulmonary toxicity of polymeric hexamethylene diisocyanate aerosols in mice. Toxicology and Applied Pharmacology 188, 154-164.

Lee, K.-W., Hailan, C., Yinhua, J., Kim, Y.-W., Chung, K.-W., 2008. Modification of soybean oil for intermediates by epoxidation, alcoholysis and amidation. Korean Journal of Chemical Engineering 25, 474-482.

Liu, Z.S., Erhan, S.Z., Xu, J.Y., 2005. Preparation, characterization and mechanical properties of epoxidized soybean oil/clay nanocomposites. Polymer 46, 10119-10127.

M. O. Okoroafor, K.C.F., 1995. Introduction to foams and foam formation, in: Landrock, A.H.E. (Ed.), Handbook of Plastic Foams. Noyes, pp. 1-10.

Mazzon, E., Habas-Ulloa, A., Habas, J.-P., 2015. Lightweight rigid foams from highly reactive epoxy resins derived from vegetable oil for automotive applications. Eur. Polym. J. 68, 546-557.

McElhanon, J.R., Russick, E.M., Wheeler, D.R., Loy, D.A., Aubert, J.H., 2002. Removable foams based on an epoxy resin incorporating reversible Diels-Alder adducts. Journal of Applied Polymer Science 85, 1496-1502.

Pampolini, G., 2010. Les propriétés mécaniques des mousses polymériques à cellules ouvertes : expériences, modèle théorique et simulations numériques, Laboratoire de Mécanique et d'Acoustique. Université de Provence, France.

Pan, X., Sengupta, P., Webster, D.C., 2011. High Biobased Content Epoxy-Anhydride Thermosets from Epoxidized Sucrose Esters of Fatty Acids. Biomacromolecules 12, 2416-2428.

Paraskevopoulou, D., Achilias, D.S., Paraskevopoulou, A., 2012. Migration of styrene from plastic packaging based on polystyrene into food simulants. Polymer International 61, 141-148.

Pauluhn, J., 2002. Short-term inhalation toxicity of polyisocyanate aerosols in rats: Comparative assessment of irritant-threshold concentrations by bronchoalveolar lavage. Inhalation Toxicology 14, 287-301.

Resnik, D.B., Elliott, K.C., 2015. Bisphenol A and risk management ethics. Bioethics 29, 182-189.

Richardson, M.O.W., 1980. FOAMS IN THE BUILDING-INDUSTRY. Plastics & Rubber International 5, 115-118.

Ruan, T., Liang, D., Song, S.J., Song, M.Y., Wang, H.L., Jiang, G.B., 2015. Evaluation of the in vitro estrogenicity of emerging bisphenol analogs and their respective estrogenic contributions in municipal sewage sludge in China. Chemosphere 124, 150-155.

Sakly, A., Laksimi, A., Kebir, H., Benmedakhen, S., 2016. Experimental and modelling study of low velocity impacts on composite sandwich structures for railway applications. Engineering Failure Analysis 68, 22-31.

Sankaran, S., Sekhar, K.R., Raju, G., Kumar, M.N.J., 2006. Characterization of epoxy syntactic foams by dynamic mechanical analysis. Journal of Materials Science 41, 4041-4046.

Schmitt, K.U., Muser, M.H., Niederer, P.F., 2003. Evaluation of a new visco-elastic foam for automotive applications. International Journal of Crashworthiness 8, 169-177.

Smardzewski, J., Grbac, I., Prekrat, S., 2008. Nonlinear mechanics of hyper elastic polyurethane furniture foams. Drvna Industrija 59, 23-28.

Stefani, P.M., Barchi, A.T., Sabugal, J., Vazquez, A., 2003. Characterization of epoxy foams. Journal of Applied Polymer Science 90, 2992-2996.

Takiguchi, O., Ishikawa, D., Sugimoto, M., Taniguchi, T., Koyama, K., 2008. Effect of rheological behavior of epoxy during precuring on foaming. Journal of Applied Polymer Science 110, 657-662.

1 Treloar, L.R.G., 1975. The physics of rubber elasticity, 3rd edition ed. Oxford University Press,
2 UK.

3 Tungare, A.V., Martin, G.C., Gotro, J.T., 1988. Chemorheological characterization of
4 thermoset cure. Polymer Engineering and Science 28, 1071-1075.

5 Zheng, J.Q., Xiang, J.W., Luo, Z.P., Ren, Y.R., 2011. Crashworthiness design of transport
6 aircraft subfloor using polymer foams. International Journal of Crashworthiness 16, 375-383.

7

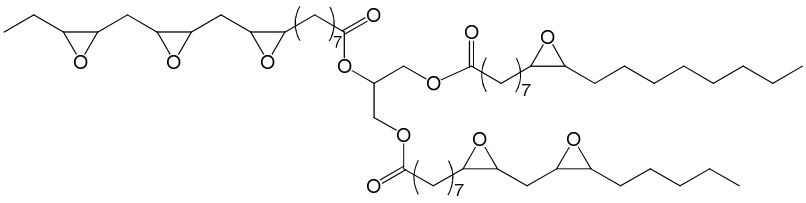

Epoxidized Linseed Oil (ELO)

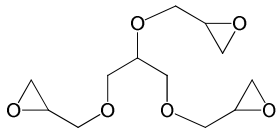

Epoxidized Glycerol (EG)

Figure 1. Epoxy prepolymers used in this study.

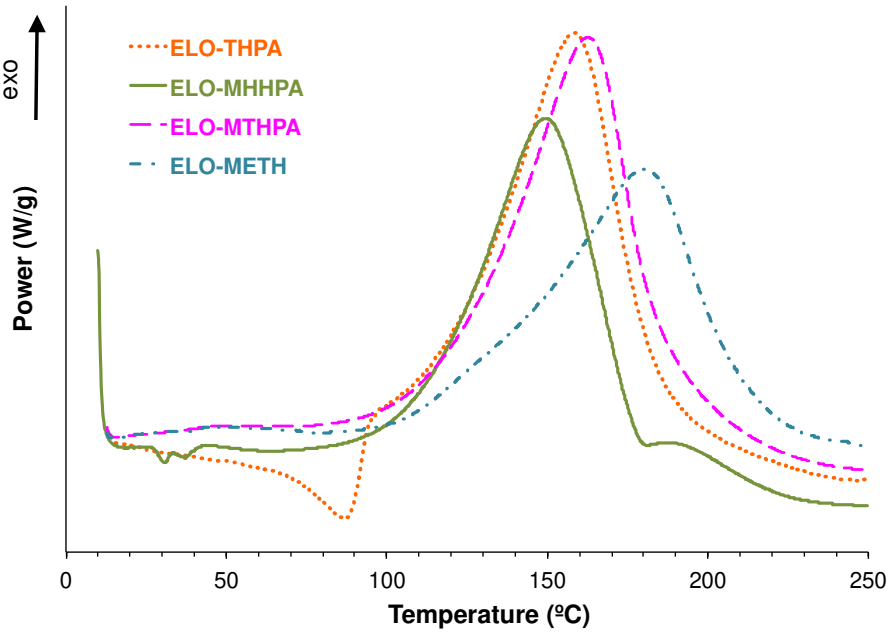

Figure 2. Dynamic DSC scans of several "ELO – anhydride" reactive mixtures performed under nitrogen with a heating rate of 5 °C min^{-1}.

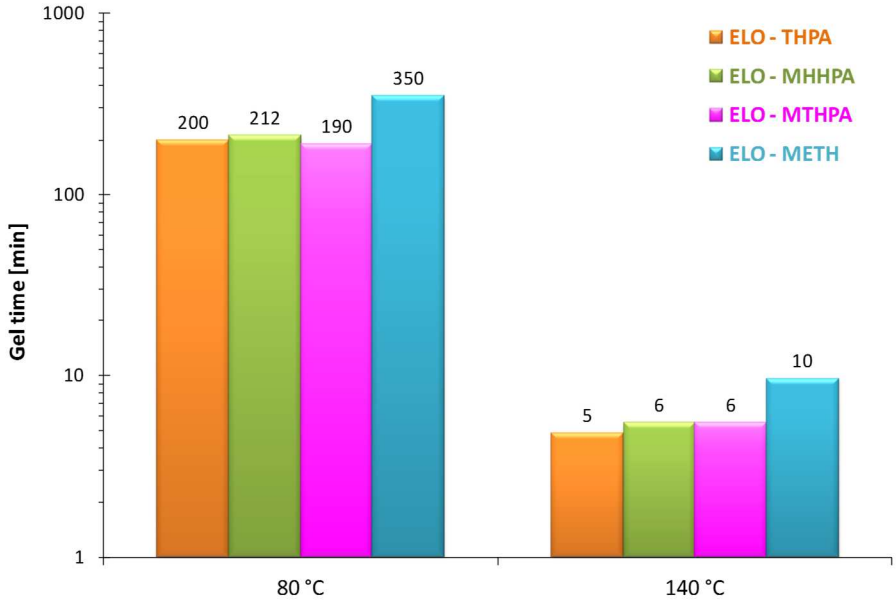

Figure 3. Gel times of several reactive mixtures "ELO – anhydride" at T = 80 °C and 140 °C.

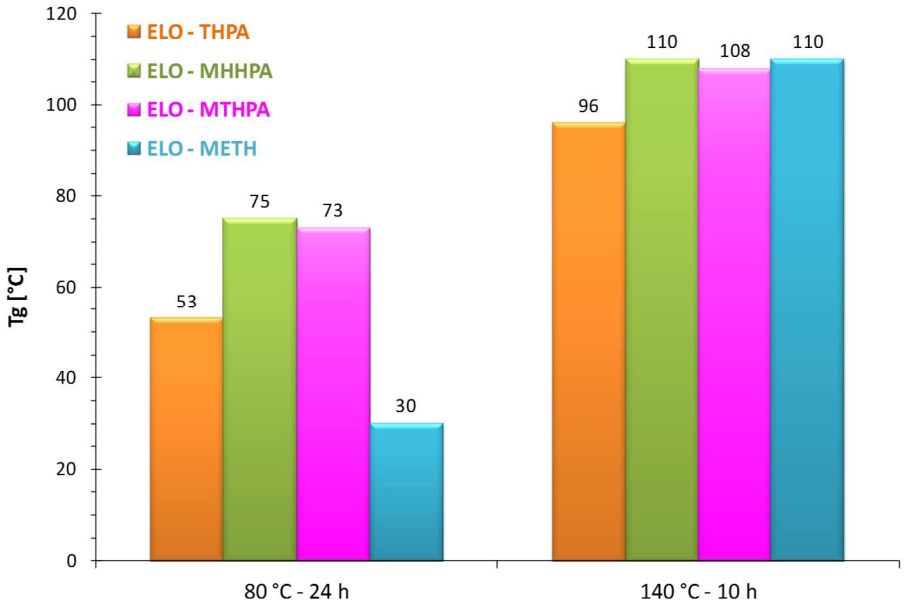

Figure 4. Glass transition temperatures of cured materials based on "ELO – anhydride" mixtures after curing at T = 80 °C during 24 hours or at T = 140 °C during 10 hours.

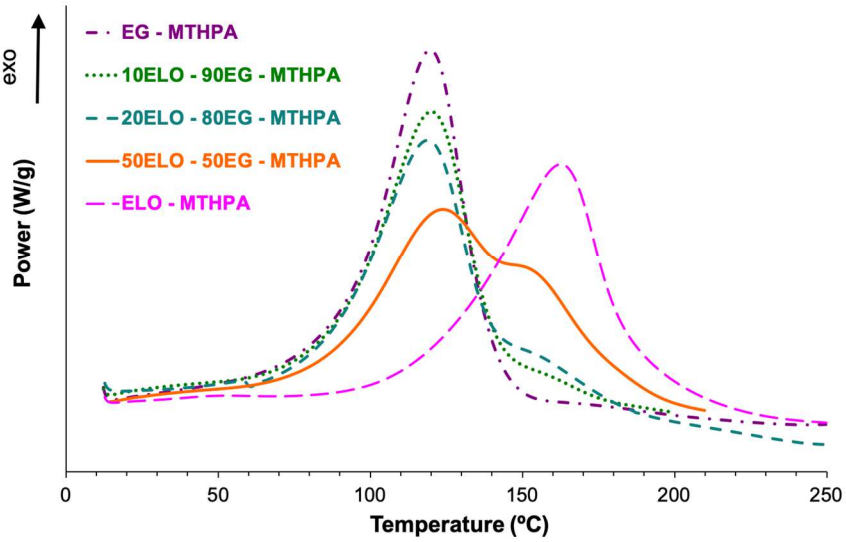

Figure 5. Dynamic DSC scans of several binary and ternary epoxy reactive mixtures performed under nitrogen with a heating rate of 5 °C min^{-1}.

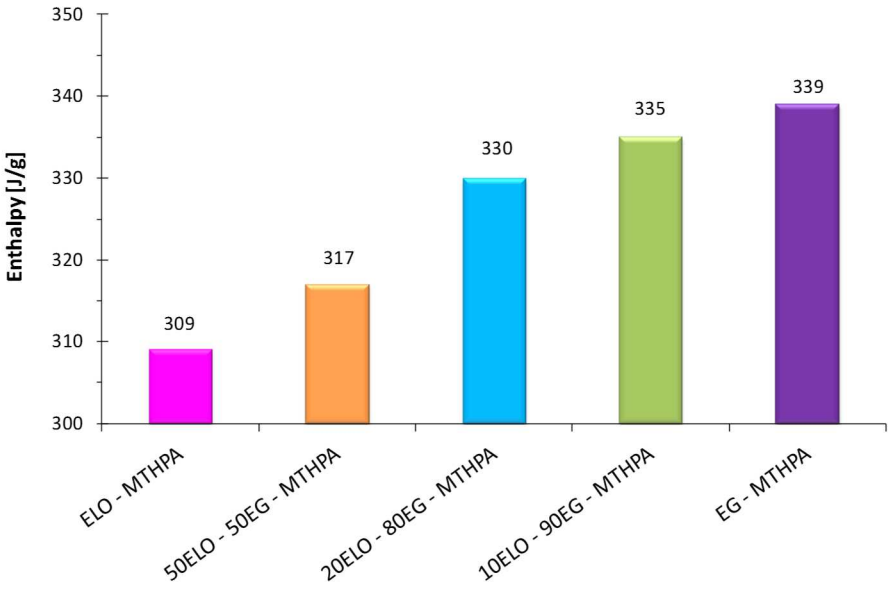

Figure 6. Influence of initial respective proportion of EG and ELO on enthalpy of crosslinking reaction released during curing.

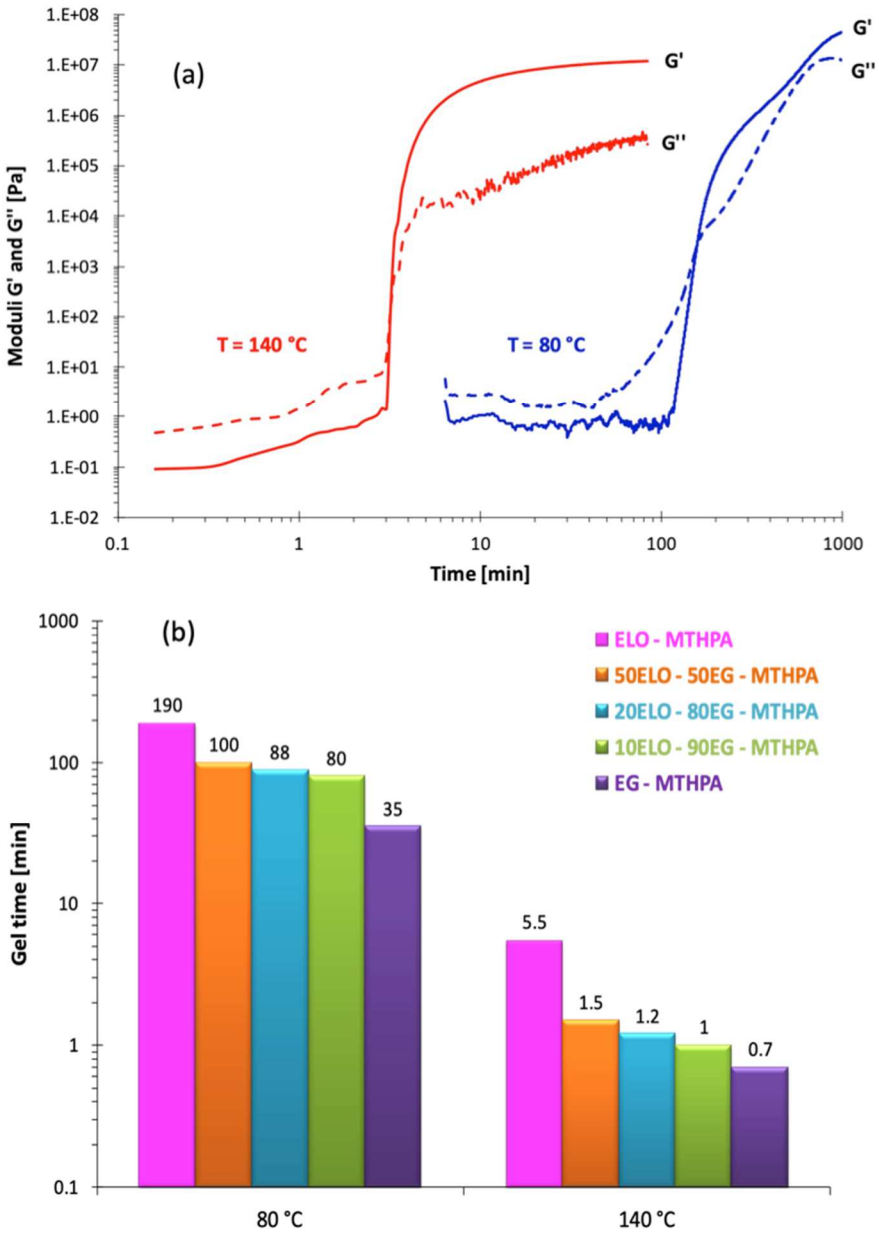

Figure 7. (a): Kinetic rheological analyses of 80ELO – 20EG – MTHPA reactive mixture and **(b):** gel times of other ternary mixtures registered at T = 80 °C and 140 °C .

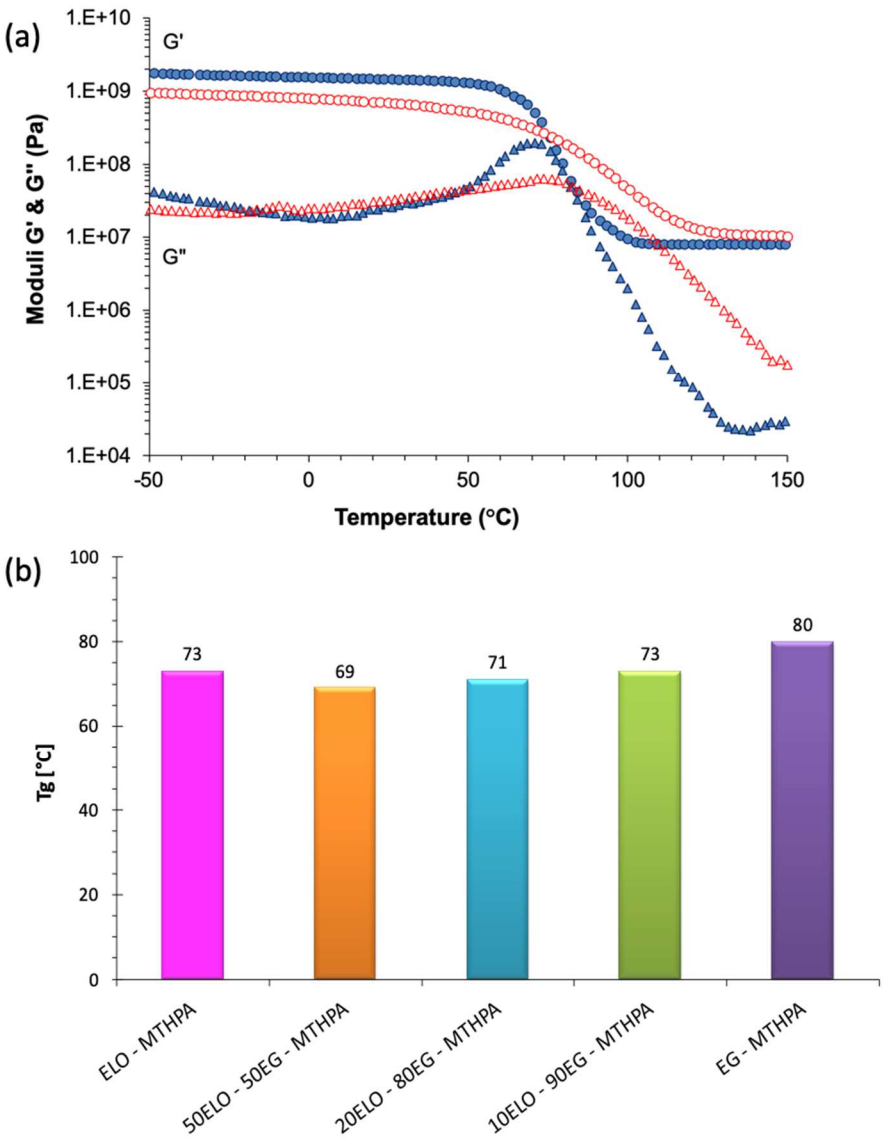

Figure 8. (a): Thermomechanical analyses of cured materials based on ELO-MTHPA (open symbols) and 10ELO – 90EG – MTHPA (full symbols) formulations.

(b): evolution of the Tg with the initial chemical composition of "xELO – (100-x)EG – MTHPA" reactive mixtures after curing.

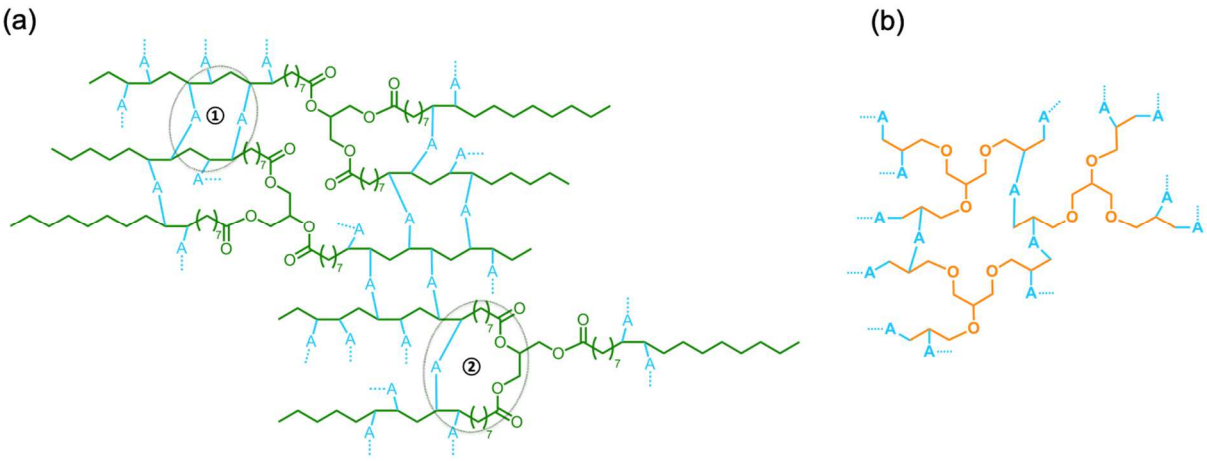

Figure 9. (a) : Representation of ELO – anhydride (A) and **(b) :** EG – anhydride networks after curing.

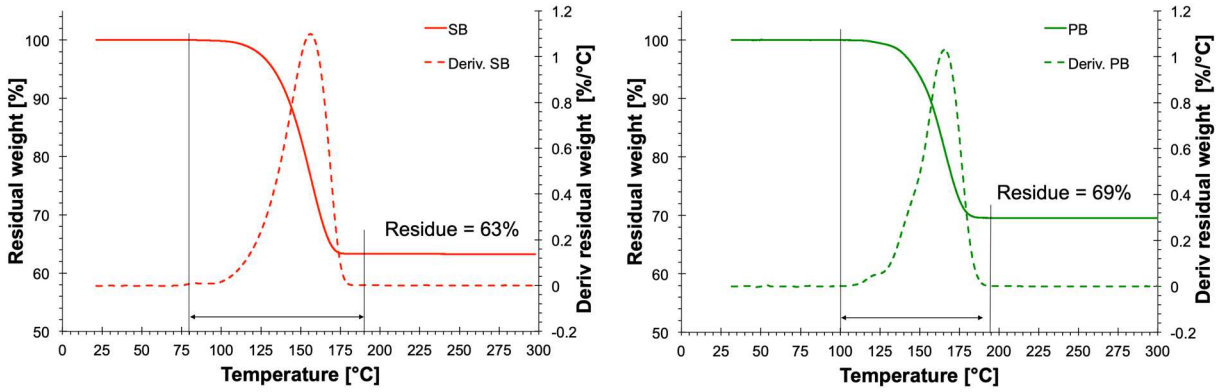

Figure 10. TGA (solid line) and DTG (dashed line) of sodium bicarbonate (left) and potassium bicarbonate (right) under air at the heating rate of 5 °C min^{-1}.

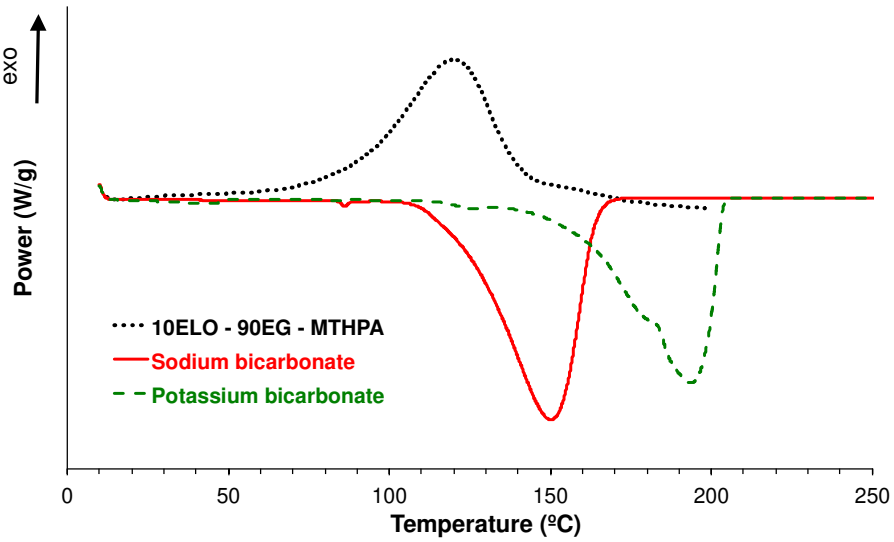

Figure 11. Dynamic DSC scans of epoxy reactive mixture and foaming agents (SB and PB) performed under nitrogen with a heating rate of 5 °C min^{-1}.

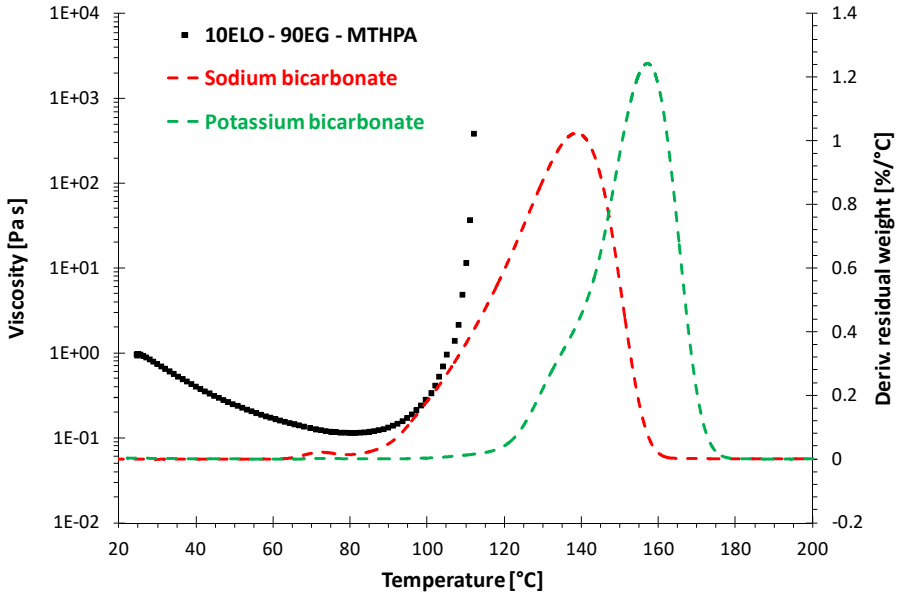

Figure 12. Epoxy reactive mixture viscosity evolution with temperature (on the left) and DTG curve of foaming agents SB and PB (on the right).

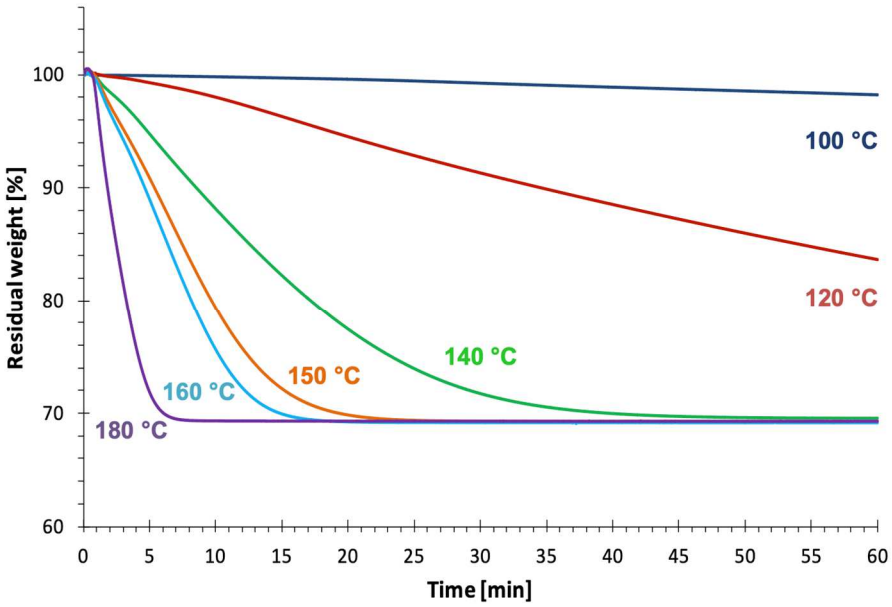

Figure 13. Isothermal TGA analyses of potassium bicarbonate under air at several temperatures between T = 100 °C and 180 °C.

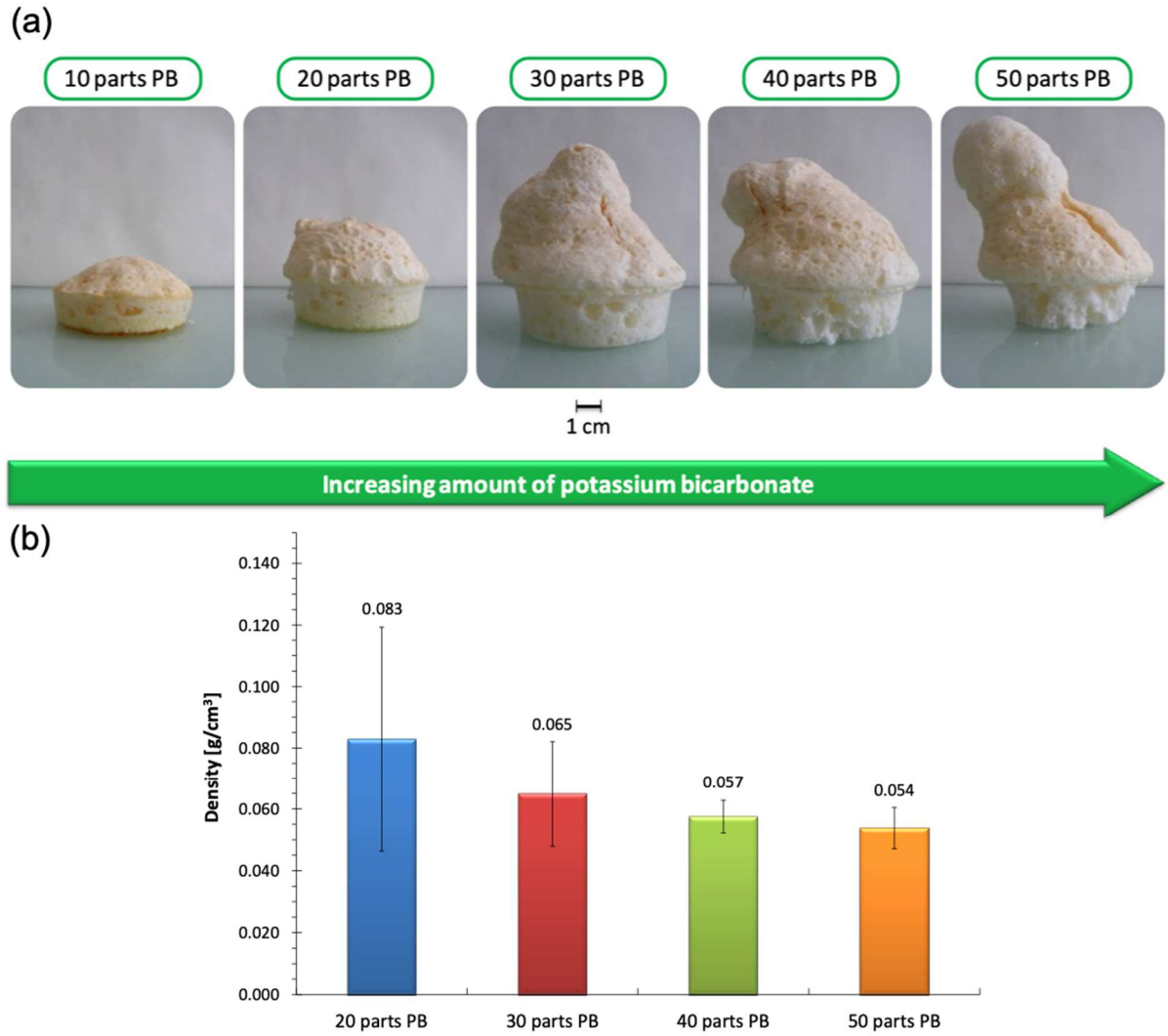

Figure 14. Overview of foams produced (during 3 minutes at T = 180 °C) with an increasing amount of foaming agent and corresponding density values.

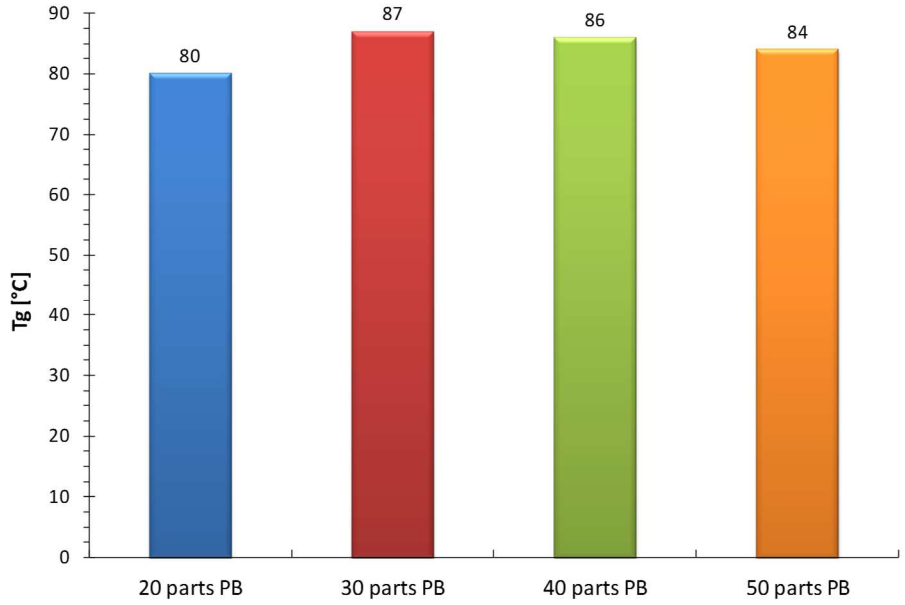

Figure 15. Tg values of foams produced during 3 minutes at T = 180 °C with an increasing amount of foaming agent.

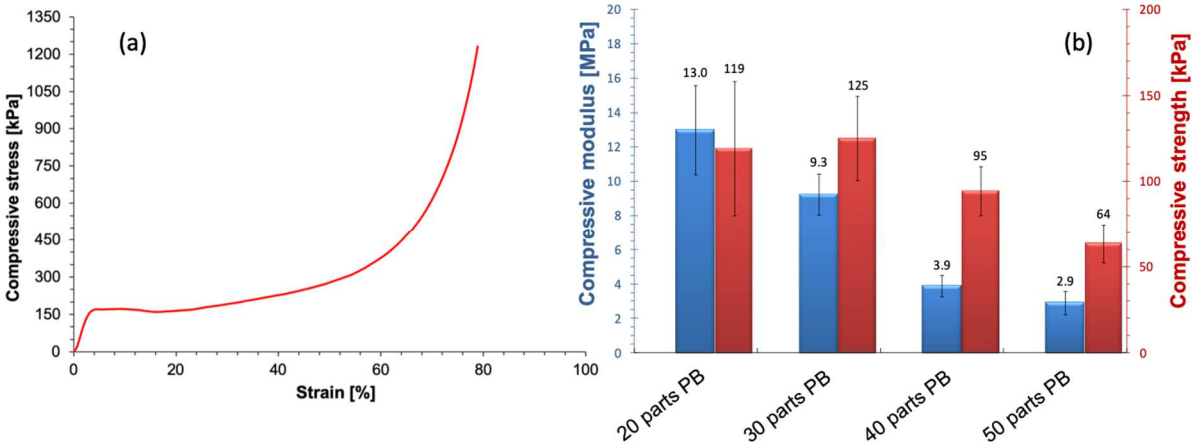

Figure 16. (a) : Compressive stress – strain curve of foam obtained in 3 minutes at T = 180 °C with 30 parts of foaming agent - (b) : Influence of foaming agent amount on compressive modulus and strength of foams produced in the same conditions.

Name	Formula	CAS number	Molecular weight (g/mol)	Melting temperature (Tm, °C)
Methyl tetrahydrophthalic anhydride (MTHPA)	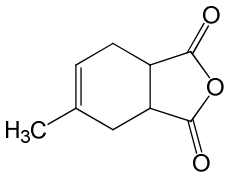	3425-89-6	166.2	-15
Tetrahydrophthalic anhydride (THPA)	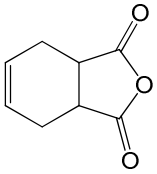	935-79-5	152.2	102
Methyl hexahydrophthalic anhydride (MHHPA)	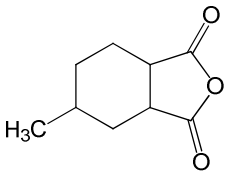	19438-60-9	168.2	-15
Nadic methyl anhydride (METH)	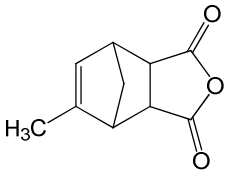	25134-21-8	178.2	-50

Table 1. Anhydride hardeners retained in this work.

Epoxidized linseed oil (ELO)

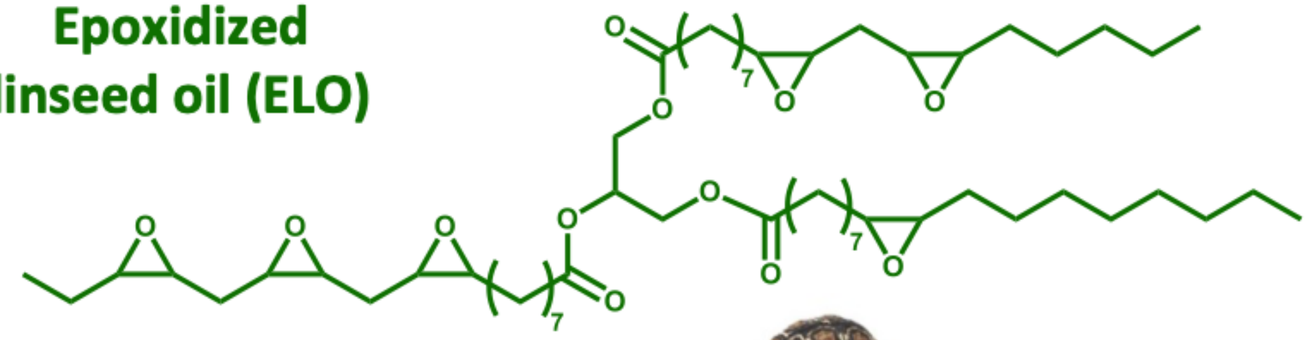

Low reactivity

Epoxidized glycerol (EG)

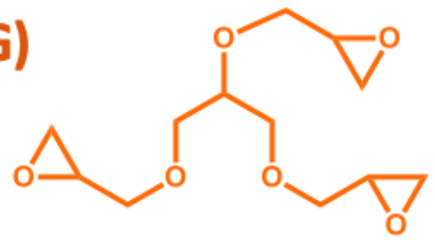

High reactivity

Ternary formulations

x ELO – (100-x) EG – hardener

Increasing amount of foaming agent